NIH Public Access
Author Manuscript
*J Child Neurol*. Author manuscript; available in PMC 2013 June 28.

Published in final edited form as:
*J Child Neurol*. 2011 September ; 26(9): 1145–1153. doi:10.1177/0883073811408308.

# MRI as a Translational Tool for the Study of Neonatal Stroke

**Mark Dzietko, MD**, **Michael Wendland, PhD**, **Nikita Derugin, MA**, **Donna M. Ferriero, MD**, and **Zinaida S. Vexler, PhD**
Department of Pediatrics, University of California, San Francisco, San Francisco, California (MD, DMF); the Department of Neurology, University of California, San Francisco, San Francisco, California (MD, ND, DMF, ZSV); and the Department of Radiology, University of California, San Francisco, California (MW).

## Abstract

More than half of neonatal stroke survivors have long-term sequelae, including seizures and neurological deficits. Although the immature brain has tremendous potential for recovery, mechanisms governing repair are essentially unexplored. We explored whether magnetic resonance imaging (MRI) early or late after transient middle cerebral arterial occlusion in 10-day-old (P10) rats can serve as an intermediate endpoint for long-term studies. Injured animals selected by diffusion-weighted MRI during middle cerebral arterial occlusion were scanned using T2-weighted MRI at P18 and P25 (injury volumes on MRI and histology were compared), or were subjected to contrast-enhanced MRI at P13 to characterize cerebral microcirculatory disturbances and blood-brain barrier leakage. Injury volume did not predict histological outcome at 2 weeks. Major reductions occurred by P18, with no further changes by P25. Cerebral perfusion was significantly reduced in the injured caudate but blood-brain barrier leakage was small. Therefore, conventional T2-weighted MRI performed during a subchronic injury phase predicts long-term histological outcome after experimental neonatal focal stroke.

### Keywords

neonate; ischemia-reperfusion; cerebral perfusion; blood-brain barrier

## Introduction

After decades of research focused on acute neuroprotection coupled with the failure of essentially all stroke clinical trials, it is questionable whether protective efforts should continue to focus on the acute injury phase. In fact, the Stroke Progress Review Group in 2006 identified brain repair after stroke as a major priority for stroke research.[1] In the immature human brain, region and cell population vulnerability depend on the age when the insult occurs. An increasing number of studies demonstrate that changes seen in the newborn on MRI at the time of injury correlate well with neurodevelopmental outcomes (reviewed in [2]). Therefore, the ability to incorporate magnetic resonance imaging (MRI) as a surrogate injury measure in preclinical studies of strategies to protect or repair the injured immature brain will enhance bench-to-bed translation.

The immature brain is very plastic, thus providing an extended window for enhancement of repair and remodeling, but the mechanisms governing repair in the injured *newborn* brain

Address correspondence to: Zinaida Vexler, PhD, Department of Neurology, 521 Parnassus Avenue, San Francisco CA 94143-0663; phone: (415) 502-2282; fax: (415) 502-5821; zena.vexler@ucsf.edu. .

The authors have no conflict of interest to report.

NIH-PA Author Manuscript
NIH-PA Author Manuscript
NIH-PA Author Manuscript

NIH-PA Author Manuscript

NIH-PA Author Manuscript

NIH-PA Author Manuscript

are essentially unexplored. The middle cerebral arterial occlusion model first developed in juvenile postnatal day 14 (P14) to P18 spontaneously hypertensive rats[3] and, later, in normotensive P7[4] and P10[5] rats, enabled studies of *focal* arterial stroke during early postnatal development. The middle cerebral arterial occlusion model is clinically relevant, as it has a reperfusion component,[6] and reperfusion is common in neonatal arterial stroke.[7] It has become clear that animals recover over time from stroke during the neonatal period, but that the extent and the timing of recovery vary substantially between individual animals. Several recent MRI studies in neonatal hypoxia-ischemia and focal stroke rodent models have demonstrated that MRI is sensitive to both early and late injury and that, as in humans, a range of injury severities can be identified noninvasively in individual animals.[8-12] Therefore, inclusion of MRI, especially in combination with other biomarkers, may help overcome a barrier to successful bench-to-bed translation of findings to enhance repair in the injured baby brain. The overall aim of this study was to obtain a better understanding of injury evolution after neonatal focal stroke and the best time to incorporate noninvasive imaging to predict injury and long-term outcome. To answer this question, we performed diffusion-weighted MRI during a transient middle cerebral arterial occlusion in P10 rats and at 2 times during the subchronic injury phase. We then compared injury volume on MRI to histology. Considering that blood-brain barrier permeability plays a key role in protecting the brain but also in limiting delivery of neuroprotectants, we used contrast-enhanced MRI to determine the state of microcirculatory disturbances and blood-brain barrier disruption during the subchronic injury phase.

## Materials and Methods

All animal experiments were approved by the Institutional Animal Care and Use Committee of the University of California, San Francisco and every effort was made to minimize animal suffering and reduce the number of animals used. Mothers were housed in a temperature- and light-controlled facility and given food and water.

### Animal Model

Sprague-Dawley dams with a dated litter of pups were purchased from Charles River Laboratories (Wilmington, Massachusetts). A transient 1.5-hour right middle cerebral arterial occlusion was performed in P10 as originally described for P7 rats[4,8] and modified for P10 rats.[13] Briefly, each pup was weighed and anesthetized with 1.5-3% isoflurane in a mixture of 70% $N_2O$ and 30% $O_2$. Temperature was maintained at 36°C to 37°C with a combination of heating blanket and overhead light. A coated 6-0 Dermalon filament was inserted into the internal carotid artery and advanced 8.5 to 9.5 mm, depending on animal size, to occlude the middle cerebral artery. The wound was closed and animals were returned to the dam. Sham controls did not have the suture advanced. Reperfusion was achieved by removing the coated filament under anesthesia, and applying gel foam to the arteriotomy in the internal carotid artery. Most pups that received middle cerebral arterial occlusion showed poor suckling during the first 2 to 3 days after surgery and were gavagefed with milk formula, with weights measured daily for 14 days to ensure adequate weight gain. Despite gavage feeding, 52% of pups did not survive over a 2-week period.

### MR Imaging

MRI was conducted at 2T (Bruker Omega CSI system, Bruker Instruments, Fremont, California) and 7T (Varian DirectDrive™ system, Varian, Inc., Palo Alto, California) to document successful occlusion of the middle cerebral artery and to characterize the ischemic injury during the first 2 weeks afterward.

NIH-PA Author Manuscript

NIH-PA Author Manuscript

NIH-PA Author Manuscript

### Diffusion-Weighted MRI

At 75 to 80 minutes after middle cerebral arterial occlusion, the entire brain was imaged with serial 2-mm thick coronal sections using diffusion-weighted imaging spin-echo echo-planar imaging to select animals with hyperintensity in the cortex and the basal ganglia, with no injury in brainstem.[6,8,13] Pups were anesthetized with isoflurane (1.5% to 2% mixed into 100% oxygen) delivered through a face mask with bite bar and modest head restraint, and wrapped in a water-recirculated warming pad to maintain core temperature. The head was positioned in a birdcage radiofrequency coil (3.3 cm diameter, 3.6 cm long) and inserted into the magnet. Reperfusion was achieved after 90 minutes of middle cerebral arterial occlusion by removing the suture under isoflurane anesthesia. Animals that exhibited ischemic injury in atypical regions such as brainstem, or with no cortical involvement, were excluded from the study.

All pups with the desired injury pattern (n = 11) were imaged at 7T on P18 and P25. We obtained T2-weighted conventional spin-echo multislice images (repetition time/echo time = 3000/50 ms) covering the entire brain with consecutive 1 mm coronal sections with field of view = 2.56 cm, and data matrix of 128×128 points (0.2 mm in-plane pixel dimension).

### Gadolinium-Diethylenetriamine Pentaacetic Acid-Enhanced T1-Weighted and Perfusion-Sensitive MRI

An additional 3 pups with confirmed diffusion-weighted imaging abnormalities during middle cerebral arterial occlusion were imaged at 2T on 3 and 7 days after reperfusion with a bolus of contrast agent and perfusion-sensitive imaging to characterize blood-brain barrier leakage and to document the extent of cerebral microcirculatory disturbances, respectively. A set of 32 gradient recalled echo-planar images was acquired at a singleslice location centered in the injury zone with repetition time/echo time = 1000/17 ms, field of view = 35 mm, matrix = 128, flip angle ~30 degrees. Gadolinium-diethylenetriamine pentaacetic acid (0.3 mmol/kg) was injected intra-jugularly over 3 seconds after acquiring 3 baseline images. Fifteen minutes after contrast administration a conventional T1-weighted spin-echo sequence was acquired with field of view = 32 mm, matrix = 128×128, repetition time/echo time = 600/15 ms, and 8 contiguous slices with thickness = 1 mm.

### MR Image Analysis

The number of hyperintense voxels on diffusion-weighted imaging acquired during middle cerebral arterial occlusion was measured and multiplied by the voxel volume in each MRI section. Size of injury was expressed as a fraction of ipsilateral brain volume, excluding midbrain and cerebellum.

For analysis of the bolus response, the signal change during the bolus passage was converted to $\Delta R2^*$ using the equation $\Delta R2^* = -\ln(SI(t)/SI(pre))/\text{echo time}$.[14,15] The $\Delta R2^*(t)$ curves were assumed proportional to contrast concentration-time curves. Parameter maps for peak $\Delta R2^*$, time-to-peak, relative cerebral blood volume (area under the concentration-time curve), mean transit time calculated as the normalized first moment of the gammavariate fit to the concentration-time curve, and relative cerebral blood flow (given by dividing relative cerebral blood volume by mean transit time) were calculated using commercially available software (MRVision, Winchester, Massachusetts). To evaluate regional perfusion parameters, regions of interest were drawn to encompass the entire basal ganglia and cortex region (excluding cingulate) on both in ipsilateral and contralateral hemispheres. Cortical regions of interest were typically 80 to 100 pixels, while basal ganglia regions of interest were 70 to 90 pixels. These regions of interest were applied to the parameter maps as well as to the dynamic image sets to obtain regional concentration-time curves and fitted parameters.

NIH-PA Author Manuscript

NIH-PA Author Manuscript

NIH-PA Author Manuscript

Assessment of injury at P18 and P25 was performed using T2-weighted imaging, as diffusion hyperintensity was resolved by P18. Volume of hypointense regions on T2-weighted imaging was measured in a set of 5 to 7 coronal image sections located between the anterior and posterior extent of the corpus callosum. Regions of interest included all pixels in ipsilateral and contralateral brain in the selected image sections, and all regions with altered T2-weighted signal. The size of hypointense regions was expressed as a percentage of total ipsilateral brain tissue in the selected sections.

### Histology

At P25 animals were anesthetized with sodium pentobarbital (100 mg/kg) and sacrificed by transcardiac perfusion with ice-cold 4% paraformaldehyde in 0.1M phosphate buffered saline (pH 7.4). Brains were carefully removed, post-fixed overnight, equilibrated in 30% sucrose in 0.1M phosphate buffered saline, and left at 4°C for a maximum of 72 hours. Serial 12 μm coronal sections were collected throughout the brain using a freezing microtome (Leica, CM1850, Bannockburn, Illinois), placed on Superfrost Plus glass slides (Fisher Scientific Publishing, Pittsburgh, Pennsylvania), and stored at −80°C until used. Each slide was prepared with 8 sections, the first of which showed corpus callosum near the anterior fornix (Figure 14, Paxinos, 5$^{th}$ edition) and each successive section was approximately 0.8 mm posterior to the preceding section, covering the brain between the anterior and posterior fornix of the corpus callosum, each of which was representative of MRI sections. Slides stained with Nissl were graded on a scale of zero to 3 [0 = no injury, 1 = few small areas of focal injury, 2 = multiple areas of focal injury, and 3 = widespread injury with loss of architecture (Nikon Optiphote-2 microscope; 20x objective)]. These 4 regional scores were summed to give a total score of 0 to 12. Brains were then classified from 0 to 4 for mild, 5 to 8 for moderate, and 9 to 12 for severe injury based on the total injury score.

### Statistical Analysis

Values are present as mean +/− SD. Statistical significance for bolus data was determined at $P < .05$ using *t*-test. Regression analysis was used to compare MRI and histological data.

## Results

### Volume of Tissue at Risk During Neonatal MCAO Does Not Predict Long-term Injury/ Recovery

The characteristic pattern of the hyperintense region on diffusion-weighted imaging that involves cortex and striatum (Figure 1A) was observed in 68% of rat pups. Consistent with our previous findings in P10 rats, [13] volume of the altered diffusion-weighted imaging signal included 60.5±7.8% of the ipsilateral hemisphere (Figure 1B).

Major reductions in the extent of injury by MRI occurred during one week after middle cerebral arterial occlusion in the surviving animals. At P18 the hypointense regions occupied 6.0±5.0% of ipsilateral brain on T2-weighted MRI, only one tenth the extent of injury evident during occlusion, and remained unchanged over the next week (6.4±4.8% at P25). The volume of injury ranged between 0 to 16.9% of total ipsilateral hemisphere volume (Figure 2), and the ipsilateral brain volume was 92.9±5.5% compared with contralateral hemisphere. The volume of injury remained essentially unchanged during the second week after middle cerebral arterial occlusion, 0 to 16.7% of total ipsilateral hemisphere volume (Figure 2B). Therefore, T2-weighted imaging delineated a significant but variable extent of injury reduction during the first week after transient middle cerebral arterial occlusion, and only modest additional changes during the second week.

NIH-PA Author Manuscript

NIH-PA Author Manuscript

NIH-PA Author Manuscript

### Cerebral Microcirculation is Disturbed but Gadolinium-Diethylenetriamine Pentaacetic Acid Uptake is Modest During Sub-chronic Injury Phase

We then asked if injury (or recovery) was associated with disturbances of cerebral microcirculation and increased blood-brain barrier permeability. Multiple parameters for gadolinium-diethylenetriamine pentaacetic acid transit through injured compared with contralateral regions were derived from ΔR2* curves (Figure 2). Given that ΔR2* is proportional to the contrast concentration in the blood, that the area under the ΔR2* curve is proportional to cerebral blood volume, and that the mean transit time taken as the first moment of the gamma variate fit to the ΔR2* curve estimates the dynamics of contrast transit, we measured relative cerebral blood volume and cerebral blood flow in injured compared with matching contralateral regions. Dynamic imaging of gadolinium-diethylenetriamine pentaacetic acid bolus showed disturbances in microcirculation in the 3 pups studied at P13 (Table 1, Figure 2). In injured cortex, although animal to animal variability and regional variability in the peak ΔR2*, relative cerebral blood volume and relative cerebral blood flow were observed, these parameters remained relatively-well preserved whereas gadolinium-diethylenetriamine pentaacetic acid bolus showed disturbances in microcirculation in the 3 pups studied at P13 (Table 1, Figure 2). In injured cortex, although animal to animal variability and regional variability in the peak ΔR2*, relative cerebral blood volume and relative cerebral blood flow were observed, these parameters remained relatively-well preserved whereas gadolinium-diethylenetriamine pentaacetic acid first-pass transit through the tissue was more variable and prolonged (Table 1). In injured caudate, the extent of disturbances was more profound than in the cortex (Table 1).

Gadolinium-diethylenetriamine pentaacetic acid-enhanced T1-weighted imaging performed as a part of the same imaging session showed no contrast leakage in the cortex. In the caudate of 2 pups (Figure 2B), the region with enhanced contrast occupied only 1.5% and 8.0 % of ipsilateral volume. A substantial improvement in cerebral perfusion was evident in the caudate of 2 of the 3 pups that survived to 7 days. Compared to that in contralateral caudate, relative cerebral blood flow increased from 0.48 to 0.75. Both of these pups also showed substantial contrast uptake on T1-weighted imaging in the caudate, including the pup that exhibited no uptake at Day 3. Cumulatively, these data demonstrate that cerebral microcirculation is disturbed in the caudate during the subchronic injury phase but this disturbance is not associated with major opening of the blood-brain barrier at this point.

### T2-Weighted MRI Predicts Histological Injury 15 Days After Neonatal Transient Middle Cerebral Arterial Occlusion

The histological injury score acquired from Nissl stained sections in the ipsilateral hemisphere at P25 ranged from 3 to 12. A regression analysis revealed a significant correlation between size of injury measured by MRI at P18 or P25 and the injury score acquired in histological sections (Figure 3).

## Discussion

Using MR imaging as a surrogate marker of outcome of transient middle cerebral arterial occlusion in P10 rats, we demonstrate here that while edema formation during occlusion does not predict histological outcome at 2 weeks, conventional T2-weighted MRI during the subchronic phase accurately demarcates histological outcome. We also show, for the first time, that perfusion deficits are present during the subchronic injury phase but that they are not associated with major opening of the blood-brain barrier.

NIH-PA Author Manuscript

NIH-PA Author Manuscript

NIH-PA Author Manuscript

We evaluated cerebral microcirculation in the postischemic brains using MR contrast bolus transit method, a semiquantitative approach based on the change in R2* relaxation rate caused by the susceptibility change in the brain during the first-pass contrast agent transit.[16] This method provides a large dynamic range of signal change and does not require measurements of the arterial input function, as the data are presented as a ratio of signal intensity changes in injured compared with matching contralateral hemisphere. The microvascular disturbances were quite diverse at 3 days after middle cerebral arterial occlusion in the 3 pups studied, providing a potential explanation for the diverse injury evident at P18 and P25.

While the relatively thick slices (2 mm) used for signal acquisition might have obscured the extent of heterogeneity, the disturbed perfusion was evident in the injured region. Cerebral perfusion was substantially more disturbed in the caudate, the ischemic core region, than in the cortex. Importantly, the associated microvascular contrast leakage was very subtle, with only minor signal enhancement in caudate evident on T1-weighted images. Although it is possible that small regions with large leakage were not revealed due to slice thickness, rather large perfusion insufficiency at 3 days was not associated with major disruption of the blood-brain barrier. The latter finding is of key importance for preclinical trial design given a frequently made assumption that therapeutic agents can easily get to injured brain through the disturbed blood-brain barrier. Rather, appropriate vehicles need to be used to deliver protective or regenerative agents across the blood-brain barrier to injured neonatal brain.

The timing of MRI acquisition plays a critical role in the ability to predict long-term injury. While diffusion-weighted imaging performed during middle cerebral arterial occlusion in neonatal rats reliably predicted injury outcome at 24 hours,[6] it did not predict one-week outcome in P7 rats after severe focal ischemic injury[8] and, as we show here, in P10 rats after a more modest ischemic injury. When performed 2 to 3 hours after reoxygenation in the hypoxia-ischemia model, diffusion-weighted imaging underestimates histological outcome 7 days later,[17-19] likely due to a transient metabolic recovery after reoxygenation. In contrast, the severity score established based on T2-weighted imaging at 24 hours after hypoxia-ischemia shows strong correlation with T2-weighted imaging, histological scoring, and behavior outcomes at 28 days.[10] We provide evidence here that while a major reduction of MRI-identifiable injury occurs during the first week following focal transient middle cerebral arterial occlusion in P10 rats, essentially no further changes on T2-weighted MRI occur over the subsequent week. Furthermore, the location and pattern of injury on T2-weighted MRI performed at P18 are similar to that by histology in all brains, demonstrating that T2-weighted imaging performed one week after injury predicts the histologic outcome at later time points. Therefore, should regenerative therapy be started at this or later timepoints, T2-weighted MRI will provide reliable information about the effects of agents administered after resolution of acute cell death.

The mechanisms underlying T2-weighted hyperintensity early and hypointensity 1 to 2 weeks after injury are not completely understood. While early ischemia-induced diffusion-weighted imaging decrease is caused, in part, by redistribution of water between the extracellular and intracellular space[20,21] and metabolic energy failure,[18,22] a transient renormalization of diffusion-weighted imaging signal occurs shortly after reperfusion and/or reoxygenation[20,21,23] and, depending on injury severity, is followed by a secondary phase of hyperintensity. Reactive astrocytosis and local inflammation are likely mechanisms that contribute to T2-weighted hyperintensity during the acute injury phase. T2 shortening (hypointensity on T2-weighted imaging) that we observed one and 2 weeks after middle cerebral arterial occlusion may occur as a result of iron or calcium deposition in the tissue upon infiltration of peripheral blood cells and gliosis. In a more severe middle cerebral arterial occlusion model in P7 rats, we previously showed a gradual and sustantial increase

NIH-PA Author Manuscript

NIH-PA Author Manuscript

NIH-PA Author Manuscript

in accumulated macrophages in the caudate and the cortex, with the peak 7 days after injury[8] but we did not determine the presence of inflammatory cells in the current study. Leukocyte infiltration through a leaky barrier would be consistent with the detectable leakage of MRI contrast agent evident at 3 days post reflow, but a subset of leukocytes may extravasate even through a relatively preserved barrier.[24]

Potential benefits from incorporating MRI in preclinical neonatal stroke trials are not limited to conventional MRI techniques. MR spectroscopy has enabled differentiation between mild and severe injury in a hypoxia-ischemia model in rodents, and thus may be useful in the search for biomarkers.[19] Studies in infants with neonatal encephalopathy have shown that conventional MRI performed early and late during the neonatal period may have different sensitivity and specificity and that lactate/N-acetylaspartate measurements by proton MR spectroscopy are informative as a surrogate endpoint in clinical trials that evaluate novel neuroprotective therapies.[25] Diffusion tensor imaging has opened new prospects for studying development of normal[26,27] and injured[19,28,29] postnatal rodent brain. Considering that the injury response in the developing brain is a complex process that evolves over time[2] and that diffusion tensor imaging has shown remarkable sensitivity in delineating injury in the human baby brain,[30,31] incorporating this technique into animal studies may further foster translation of regenerative strategies for neonatal stroke.

To summarize, the combination of different imaging techniques provides the potential to improve our understanding of the complex changes that occur in the evolution of neonatal stroke and should help in the evaluation of new treatment options.

## Acknowledgments

Presented at the Neurobiology of Disease in Children Symposium: Cerebrovascular Disease, in conjunction with the 39th Annual Meeting of the Child Neurology Society, Providence, Rhode Island, October 13, 2010. Supported by grants from the National Institutes of Health (5R13NS040925-09), the National Institutes of Health Office of Rare Diseases Research, the Child Neurology Society, and the Children's Hemiplegia and Stroke Association. This study was supported by NS35902 (DMF and ZSV) and NS44025 (ZV). The authors have no conflict of interest to report. They wish to thank Melanie Fridl Ross, MSJ, ELS, for editing assistance.

## References

1. Grotta JC, Jacobs TP, Koroshetz WJ, Moskowitz MA. Stroke program review group: An interim report. Stroke. 2008; 39:1364–1370. [PubMed: 18309142]
2. Ferriero DM, Miller SP. Imaging selective vulnerability in the developing nervous system. J Anat. 2010; 217:429–435. [PubMed: 20408904]
3. Ashwal S, Cole DJ, Osborne S, et al. A new model of neonatal stroke: Reversible middle cerebral artery occlusion in the rat pup. Pediatr Neurol. 1995; 12:191–196. [PubMed: 7619184]
4. Derugin N, Ferriero DM, Vexler ZS. Neonatal reversible focal cerebral ischemia: A new model. Neurosci Res. 1998; 32:349–353. [PubMed: 9950062]
5. Mu D, Jiang X, Sheldon RA, et al. Regulation of hypoxia-inducible factor 1alpha and induction of vascular endothelial growth factor in a rat neonatal stroke model. Neurobiol Dis. 2003; 14:524–534. [PubMed: 14678768]
6. Derugin N, Wendland M, Muramatsu K, et al. Evolution of brain injury after transient middle cerebral artery occlusion in neonatal rat. Stroke. 2000; 31:1752–1761. [PubMed: 10884483]
7. Ferriero DM. Neonatal brain injury. N Engl J Med. 2004; 351:1985–1995. [PubMed: 15525724]
8. Derugin N, Dingman A, Wendland M, et al. Magnetic resonance imaging as a surrogate measure for histological sub-chronic endpoint in a neonatal rat stroke model. Brain Res. 2005; 1066:49–56. [PubMed: 16336947]
9. Wendland MF, Faustino J, West T, et al. Early diffusion-weighted MRI as a predictor of caspase-3 activation after hypoxic-ischemic insult in neonatal rodents. Stroke. 2008; 39:1862–1868. [PubMed: 18420950]

NIH-PA Author Manuscript

NIH-PA Author Manuscript

NIH-PA Author Manuscript


10. Recker R, Adami A, Tone B, et al. Rodent neonatal bilateral carotid artery occlusion with hypoxia mimics human hypoxic-ischemic injury. J Cereb Blood Flow Metab. 2009; 29:1305–1316. [PubMed: 19436315]
11. Ashwal S, Obenaus A, Snyder EY. Neuroimaging as a basis for rational stem cell therapy. Pediatr Neurol. 2009; 40:227–236. [PubMed: 19218036]
12. Ashwal S, Tone B, Tian HR, et al. Serial magnetic resonance imaging in a rat pup filament stroke model. Exp Neurol. 2006; 202:294–301. [PubMed: 16876160]
13. Shimotake J, Derugin N, Wendland M, et al. Vascular endothelial growth factor receptor-2 inhibition promotes cell death and limits endothelial cell proliferation in a neonatal rodent model of stroke. Stroke. 2010; 41:343–349. [PubMed: 20101028]
14. Moseley ME, Vexler Z, Asgari HS, et al. Comparison of gd- and dy-chelates for t2 contrast-enhanced imaging. Magn Reson Med. 1991; 22:259–264. discussion 265-257. [PubMed: 1812356]
15. Kucharczyk J, Vexler ZS, Roberts TP, et al. Echo-planar perfusion-sensitive mr imaging of acute cerebral ischemia. Radiology. 1993; 188:711–717. [PubMed: 8351338]
16. Moseley ME, Wendland MF, Kucharczyk J. Magnetic resonance imaging of diffusion and perfusion. Top Magn Reson Imaging. 1991; 3:50–67. [PubMed: 2054198]
17. Wendland MF, Faustino J, West T, et al. Early diffusion-weighted mri as a predictor of caspase-3 activation after hypoxic-ischemic insult in neonatal rodents. Stroke. 2008; 39:1862–1868. [PubMed: 18420950]
18. van de Looij Y, Chatagner A, Huppi PS, et al. Longitudinal mr assessment of hypoxic ischemic injury in the immature rat brain. Magn Reson Med. 2010; 65:305–312. [PubMed: 20859997]
19. Wang S, Wu EX, Cai K, Lau HF, et al. Mild hypoxic-ischemic injury in the neonatal rat brain: Longitudinal evaluation of white matter using diffusion tensor mr imaging. AJNR Am J Neuroradiol. 2009; 30:1907–1913. [PubMed: 19749219]
20. Dijkhuizen RM, de Graaf RA, Tulleken KA, Nicolay K. Changes in the diffusion of water and intracellular metabolites after excitotoxic injury and global ischemia in neonatal rat brain. J Cereb Blood Flow Metab. 1999; 19:341–349. [PubMed: 10078886]
21. Qiao M, Malisza KL, Del Bigio MR, Tuor UI. Transient hypoxia-ischemia in rats: Changes in diffusion-sensitive mr imaging findings, extracellular space, and na+-k+ - adenosine triphosphatase and cytochrome oxidase activity. Radiology. 2002; 223:65–75. [PubMed: 11930049]
22. Dijkhuizen RM, van Lookeren Campagne M, Niendorf T, et al. Status of the neonatal rat brain after nmda-induced excitotoxic injury as measured by mri, mrs and metabolic imaging. NMR Biomed. 1996; 9:84–92. [PubMed: 8887373]
23. Rumpel H, Nedelcu J, Aguzzi A, Martin E. Late glial swelling after acute cerebral hypoxia-ischemia in the neonatal rat: A combined magnetic resonance and histochemical study. Pediatr Res. 1997; 42:54–59. [PubMed: 9212037]
24. Ransohoff RM, Kivisakk P, Kidd G. Three or more routes for leukocyte migration into the central nervous system. Nat Rev Immunol. 2003; 3:569–581. [PubMed: 12876559]
25. Thayyil S, Chandrasekaran M, Taylor A, et al. Cerebral magnetic resonance biomarkers in neonatal encephalopathy: A meta-analysis. Pediatrics. 2010; 125:e382–e395. [PubMed: 20083516]
26. Mori S, Zhang J. Principles of diffusion tensor imaging and its applications to basic neuroscience research. Neuron. 2006; 51:527–539. [PubMed: 16950152]
27. Song SK, Kim JH, Lin SJ, et al. Diffusion tensor imaging detects age-dependent white matter changes in a transgenic mouse model with amyloid deposition. Neurobiol Dis. 2004; 15:640–647. [PubMed: 15056472]
28. Stone BS, Zhang J, Mack DW, et al. Delayed neural network degeneration after neonatal hypoxia-ischemia. Ann Neurol. 2008; 64:535–546. [PubMed: 19067347]
29. Drobyshevsky A, Derrick M, Wyrwicz AM, et al. White matter injury correlates with hypertonia in an animal model of cerebral palsy. J Cereb Blood Flow Metab. 2007; 27:270–281. [PubMed: 16736047]
30. Partridge SC, Mukherjee P, Berman JI, et al. Tractography-based quantitation of diffusion tensor imaging parameters in white matter tracts of preterm newborns. J Magn Reson Imaging. 2005; 22:467–474. [PubMed: 16161075]

NIH-PA Author Manuscript

NIH-PA Author Manuscript

NIH-PA Author Manuscript

31. Barkovich AJ, Miller SP, Bartha A, et al. MR imaging, MR spectroscopy, and diffusion tensor imaging of sequential studies in neonates with encephalopathy. AJNR Am J Neuroradiol. 2006; 27:533–547. [PubMed: 16551990]

NIH-PA Author Manuscript
NIH-PA Author Manuscript
NIH-PA Author Manuscript



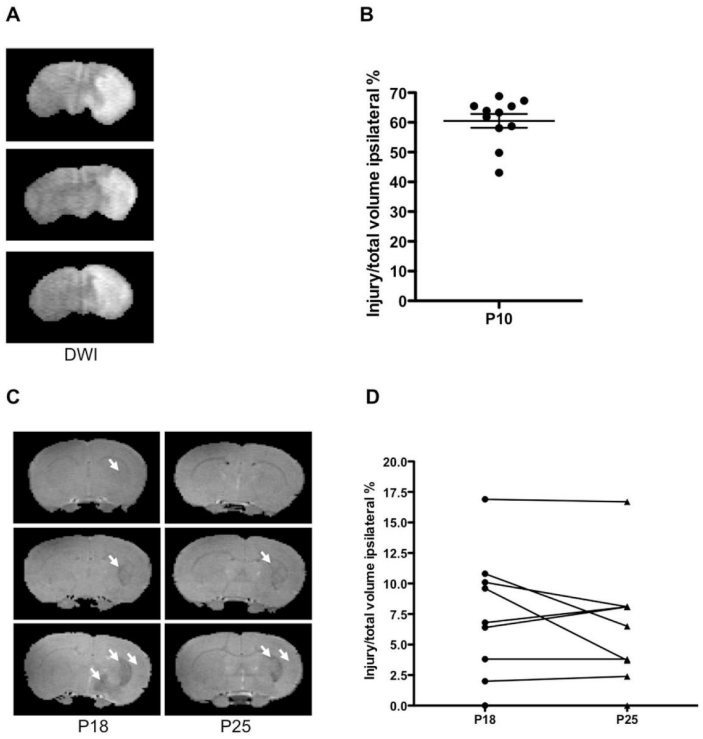


**Figure 1.**

MRI delineation of injury evolution. (A-B). Diffusion-weighted imaging during middle cerebral arterial occlusion demonstrates consistent injury pattern. (A) Representative images of 3 P10 rat pups during middle cerebral arterial occlusion. (B) The volume of tissue with affected diffusion-weighted imaging. Mean +/− SEM, n = 11. (C-D). T2-weighted injury evolution during the subchronic injury phase. (A) Examples of mild (top), moderate (middle), and severe (bottom) injury after one and 2 weeks after middle cerebral arterial occlusion. Arrows point to hypointense regions. (B) A major reduction in injury volume occurs during one week after middle cerebral arterial occlusion. Injury varies in individual animals.

NIH-PA Author Manuscript

NIH-PA Author Manuscript

NIH-PA Author Manuscript

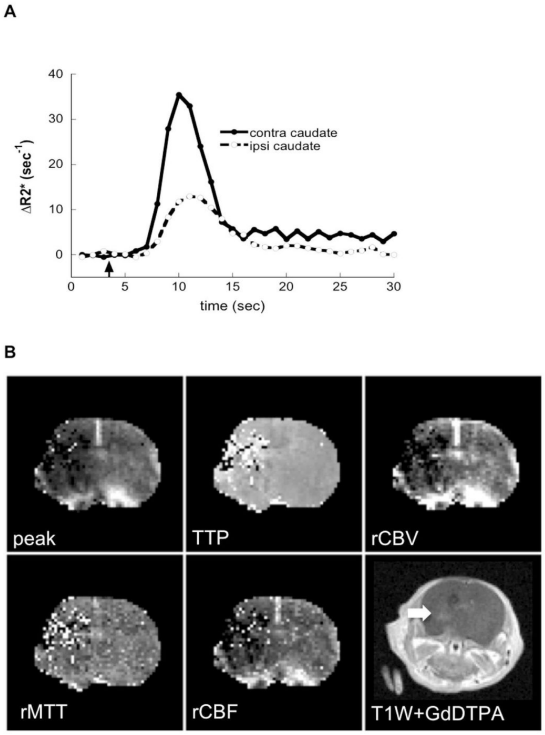


**Figure 2.**

Disturbances of cerebral microcirculation and blood-brain barrier permeabity 3 days after middle cerebral arterial occlusion. (A) ΔR2* time curves obtained before, during, and after a bolus of gadolinium-diethylenetriamine pentaacetic acid from the entire injured region of the ipsilateral hemisphere and a similar region in the contralateral hemisphere. (B) Representative images of ΔR2* (peak), time of contrast arrival relative cerebral blood volume transit time, and relative cerebral blood flow obtained in the same animal. (C) T1-weighted spin-echo images obtained 15 minutes after administration of 0.3 mmol/kg gadolinium-diethylenetriamine pentaacetic acid at the same slice locations as used for bolus response profiles. Two out of 3 pups exhibited contrast enhancement (arrows).

NIH-PA Author Manuscript

NIH-PA Author Manuscript

NIH-PA Author Manuscript

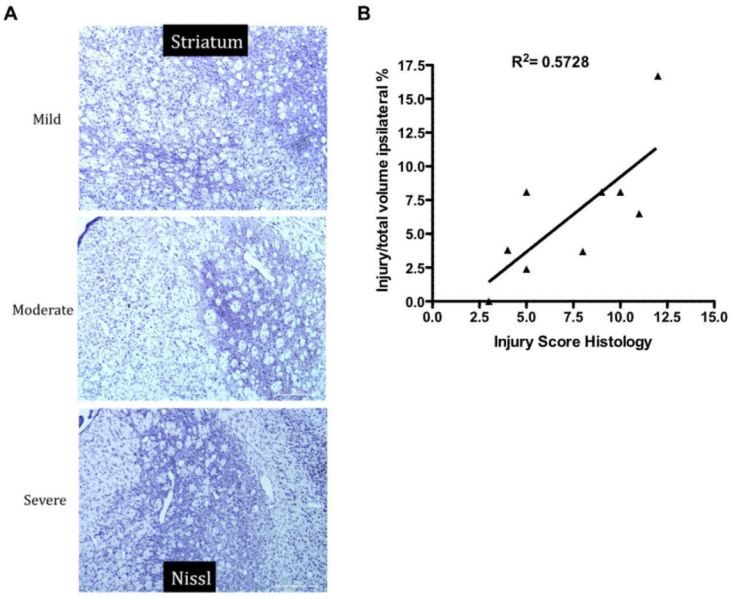


**Figure 3.**

T2-weighted imaging during subchronic injury predicts histological outcome 2 weeks after middle cerebral arterial occlusion at P10. (A) Representative Nissl-stained images of the striatum at P25. (B) A regression analysis comparing injury identified noninvasively on T2-weighted imaging to histological injury score revealed a significant correlation between these 2 parameters (D). (n = 9, $R^2 = 0.5728$, $P < .02$).

NIH-PA Author Manuscript
NIH-PA Author Manuscript
NIH-PA Author Manuscript



## Table 1

Cerebral Microcirculation Three Days After Transient MCAO at P10

| | **Peak ΔR2* (ipsi/contra)** | **Δtime-to peak (ipsi-contra)** | **rCBV (ipsi/contra)** | **ΔMTT (ipsi-contra)** | **rCBF (ipsi/contra)** |
|---|---|---|---|---|---|
| Caudate | 0.45±0.21<br>*P* = .012 | 0.80±0.60 | 0.56±0.13<br>*P* = .027 | 0.53±0.61 | 0.46±0.15<br>*P* = .005 |
| Cortex | 0.74±0.18<br>*P* = .09 | 0.95±0.31<br>*P* = .033 | 0.89±0.13 | 0.78±0.21<br>*P* = .021 | 0.66±0.13<br>*P* = .081 |

Values for peak ΔR2*, relative cerebral blood volume and relative cerebral blood flow are ratios of values obtained from regions of interest in ipsilateral/contralateral. Δtime-to-peak and Δmean transit time values are the values measured in regions of interest (ipsilateral minus contralateral regions).

Animals showed reduced perfusion in the ipsilateral brain on dynamic imaging of bolus transit (n = 3). *P* values are obtained by *t*-test.

Abbreviations: CBV, cerebral blood volume, MCAO, middle cerebral artery obstruction; MTT, mean transit time, rCBF, regional blood flow volume; rCBV. regional cerebral blood volume.